Foldamers

International Edition: DOI: 10.1002/anie.201504248
German Edition: DOI: 10.1002/ange.201504248

A Hollow Foldecture with Truncated Trigonal Bipyramid Shape from the Self-Assembly of an 11-Helical Foldamer

*Jae-Hoon Eom, Jintaek Gong, Sunbum Kwon, Aram Jeon, Rokam Jeong, Russell W. Driver, and Hee-Seung Lee**

Abstract: *The creation of self-assembling microscale architectures that possess new and useful physical properties remains a significant challenge. Herein we report that an 11-helical foldamer self-assembles in a controlled manner to form a series of 3D foldectures with unusual three-fold symmetrical shapes that are distinct from those generated from 12-helical foldamers. The foldamer packing motif was revealed by powder X-ray diffraction technique, and provides an important link between the molecular-level symmetry and the microscale morphologies. The utility of foldectures with hollow interiors as robust and well-defined supramolecular hosts was demonstrated for inorganic, organic, and even protein guests. This work will pave the way for the design of functional foldectures with greater 3D shape diversity and for the development of biocompatible delivery vehicles and containment vessels.*

Foldectures are a new class of crystalline peptidic material with unprecedented topological complexity derived from the rapid and non-equilibrium aqueous phase self-assembly of foldamers. We have demonstrated that it is feasible to obtain a variety of three-dimensional (3D) foldecture shapes from a set of β-peptide foldamers with identical 12-helical secondary structures by simple variation of the self-assembly conditions.[1] A notable architectural feature shared by these assemblies is the presence of a common four-fold symmetry axis despite the different and unusual 3D shapes, such as windmill, petal, square bar, molar tooth, and rectangular tube. This observation raised the fundamental question of whether 4-fold symmetry is intrinsic to foldectures or is instead determined by foldamer secondary structure, with new and useful foldecture morphologies potentially available through the choice of a different foldamer secondary structure. Such a relationship, if present, would offer a general and useful method to design foldectures using foldamer secondary structure as the basic unit, with specific shapes and diverse functions that more closely resemble biological architectures. To this end, among the many helical foldamers reported to date,[2] we decided to investigate the self-assembly characteristics of **1**, an α/β-heptamer composed of *trans*-(*S*,*S*)-2-aminocyclopentanecarboxylic acid (*trans*-(*S*,*S*)-ACPC) and 2-aminoisobutyric acid (Aib) monomers in an 1:1 alternating sequence, as this heterogeneous backbone is known to adopt an 11-helical conformation in both the solid and solution states through hydrogen bonding between the C=O (*i*) and N–H (*i*+3) groups (Figure 1a; Supporting Information, Figure S1).[3]

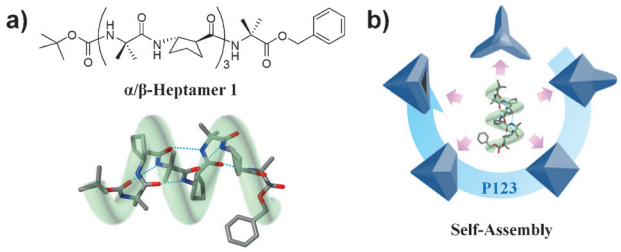

Figure 1. a) Chemical structure (top) and 11-helical molecular model (bottom) of α/β-heptamer **1**. The 11-helix pattern is so-named to reflect the number of atoms in the ring formed by backbone hydrogen bonding. b) Illustrations of various microstructures having 3-fold symmetry derived from the self-assembly of α/β-heptamer **1**.

Bacterial microcompartments (BMCs) are structurally well-defined protein shells that can enclose functional guests, such as metabolic systems or enzymes, in their void spaces.[4] The primary functions of these biological containers are to sequester and protect their guests against environmental shocks such as lethal chemicals or biological agents. BMCs often form polyhedral 3D shapes with triangular faces in which structurally well-defined protein subunits are self-assembled.[5] Owing to the intriguing structure and function of these biological architectures, several studies have sought not only to unravel the principles underlying the self-assembly mechanism,[6] but to mimic the formation of BMC-like assemblies by computer-aided de novo design, the engineering of protein subunits,[7,8] or by employing non-protein scaffolds such as coiled-coil α-peptides,[9] β-sheet-forming α-peptides,[10] and rigid aromatic amphiphiles.[11] Foldamers would be expected to be an excellent alternative substrate, but no example has been reported to date, presumably because the design principles that underlie the construction of polyhedral shapes and the encapsulation of guest molecules are not sufficiently well understood.

Herein we report that an 11-helical heptameric foldamer self-assembles in a controlled manner to form a series of 3D foldectures with unusual three-fold symmetrical shapes (Figure 1b), one of which has a void space capable of enclosing

[*] J.-H. Eom, J. Gong, Dr. S. Kwon, Dr. A. Jeon, R. Jeong, Dr. R. W. Driver, Prof. Dr. H.-S. Lee
Department of Chemistry, KAIST
Molecular-Level Interface Research Center
291 Daehak-ro, Yuseong-gu, Daejeon 305-701 (Korea)
E-mail: hee-seung_lee@kaist.ac.kr
Homepage: http://hslee.kaist.ac.kr

Supporting information for this article is available on the WWW under http://dx.doi.org/10.1002/anie.201504248.

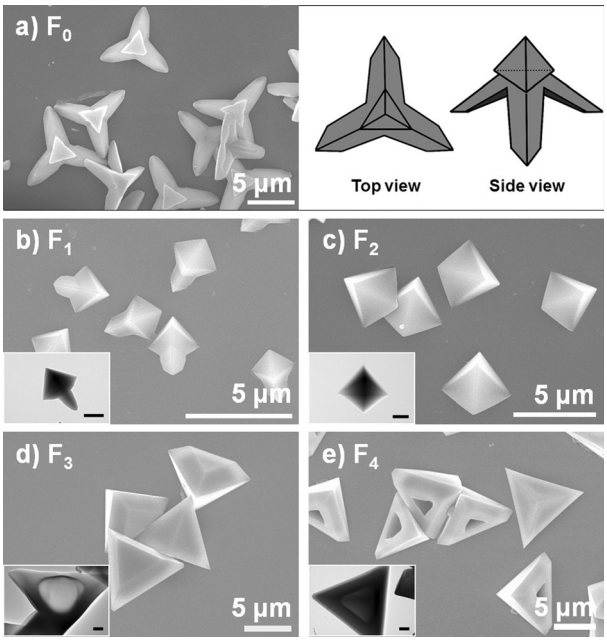

Figure 2. SEM images of foldectures derived from self-assembly of α/β-heptamer **1**: a) tripod $\mathbf{F_0}$ (right, representations) from distilled water; b) caudate trigonal bipyramid $\mathbf{F_1}$; c) trigonal bipyramid $\mathbf{F_2}$; d) truncated trigonal bipyramid $\mathbf{F_3}$; and e) truncated trigonal bipyramid with caved face $\mathbf{F_4}$ obtained from P123 concentrations of 8, 24, 40, and 48 $g\,L^{-1}$, respectively. TEM images (scale bars: 1 μm) of each foldecture are shown in the insets of b)-e).

different types of molecular guests in a way reminiscent of a BMC. This is the first example of a foldamer-based large molecular container. The foldamer packing motif was revealed by powder X-ray diffraction (PXRD) techniques and provides a molecular-level explanation for the microscale morphologies.

Upon addition of a solution of α/β-peptide **1** (200 μL, 2 $g\,L^{-1}$ in THF) to distilled water (1 mL) with vigorous stirring, a white precipitate immediately formed. Scanning electron microscopy (SEM) of the resulting foldectures showed a uniform foldecture $\mathbf{F_0}$ with a tripod shape and C_{3v} symmetry (Figure 2a; Supporting Information, Figure S2). Self-assembly studies of **1** at different peptide concentrations suggested that the tripod shape of $\mathbf{F_0}$ originates from the anisotropic growth of legs at the basal vertices (Figure S3a). That is, the molecular association rate at the apex of the trigonal pyramid seemed to be sluggish compared to the basal face apexes, resulting in a tripodal, rather than tetrapodal morphology. This phenomenon was magnified as the peptide concentration was increased (Figure S3d). It is worth noting that self-assembly studies in distilled water of both 11- and 12-helical foldamers show the formation of unusual branched shapes (tripod and windmill, respectively) with high uniformity in shape and size.[1a] However, there exist fundamental morphological differences in the microscale shapes selected by each secondary structure. The 11-helix provided only nonplanar, 3-fold symmetrical tripod shapes, whereas the 12-helix offered only planar, 4-fold symmetrical windmill shapes.

In analogy with our previous studies with 12-helical β-peptides, we then systematically investigated the effects of a nonionic surfactant, P123 (Pluronic 123, EG_{20}-PG_{70}-EG_{20}, average MW ≈ 5800), on foldecture morphology.[1] As the concentration of P123 was increased, an evolution in foldecture shapes away from the primitive shape $\mathbf{F_0}$ was observed. Figure 2b–e illustrates the SEM images of foldectures $\mathbf{F_{1\text{-}4}}$ obtained from the self-assembly of **1** at P123 concentrations of 8, 24, 40, and 48 $g\,L^{-1}$, respectively. The corresponding 3D morphologies can be described as caudate trigonal bipyramids ($\mathbf{F_1}$), trigonal bipyramids ($\mathbf{F_2}$), truncated trigonal bipyramids ($\mathbf{F_3}$), and truncated trigonal bipyramids with a concave basal facet ($\mathbf{F_4}$). $\mathbf{F_1}$–$\mathbf{F_4}$ share a common trigonal bipyramid skeleton from which morphological features are derived. In $\mathbf{F_1}$ a tail protrudes from the apex of the trigonal bipyramid while the compressed shapes and presence of basal faces in $\mathbf{F_3}$ and $\mathbf{F_4}$ were presumed to result from the inhibition of growth at the same apex. Unexpectedly and more interestingly, the transmission electron microscopy (TEM) analysis of the foldectures revealed clearly that jewel-like $\mathbf{F_3}$ is hollow, with a huge interior void space similar to a BMC.

Thus the evolution in foldecture morphology is dependent upon P123 concentration and results from the uneven effect of P123 on growth rates along the axial and equatorial directions of the trigonal bipyramid. In the absence of P123, the 11-helical foldamer self-assembled to give the primitive tripod shape $\mathbf{F_0}$ with a preferential growth rate in the equatorial direction, especially along the edges of trigonal pyramid. The presence of P123 suppresses the growth rate along the equatorial direction, thereby increasing the relative growth rate in the axial direction to give trigonal bipyramids $\mathbf{F_{1\text{-}4}}$. When the axial and equatorial growth rates are well-balanced, a perfect trigonal bipyramid $\mathbf{F_2}$ was formed. When they are unbalanced, protruded ($\mathbf{F_1}$) or truncated ($\mathbf{F_3}$ and $\mathbf{F_4}$) versions of a trigonal bipyramid were formed.

To further examine 3D shape evolution in foldectures, we carried out a comprehensive set of self-assembly experiments at different P123 and **1** concentrations. The results are illustrated in the foldecture shape diagram (Figure S6), which allows us to both predict and choose the desired 3D shape.

The unique trigonal bipyramid-based morphologies of $\mathbf{F_{0\text{-}4}}$ are presumed to arise from symmetry elements present within the molecular packing motif. In a preliminary effort to identify molecular-level structural differences within $\mathbf{F_{0\text{–}4}}$, we collected powder diffraction data for $\mathbf{F_{0\text{–}4}}$ using a standard laboratory X-ray diffractometer and found that two theta (2θ) values for foldectures $\mathbf{F_{0\text{–}4}}$ were indistinguishable within experimental error (Figure S7), confirming that all the foldectures have almost identical molecular packing motifs despite significant differences in their 3D shapes. This result also strongly supports the role of P123 as a structural determinant in the self-assembly process. P123 differentially alters the rate of molecular association, which in turn results in a diversity of macroscopic morphologies despite the preference for a single molecular packing motif.

To elucidate the molecular packing motif of the foldecture in detail at the atomic level, we carried out synchrotron PXRD pattern analysis according to our structure determination procedure by using Le Bail fitting and Rietveld refinement (Figures S8 and S9).[1b,12,13] As expected from the

2θ value comparison discussed above, PXRD analysis is consistent with identical unit cells for $\mathbf{F}_{0-4}$. Detailed crystallographic parameters, especially for foldecture $\mathbf{F}_1$ used for the designation of molecular packing orientation (see below), are listed in Table S1. The foldecture unit cell (a, $b = 14.4259$ Å; $c = 21.0815$ Å; α, $\beta = 90°$, $\gamma = 120°$) has three equivalent molecules in the $P3_2$ space group, which is different from the single crystal X-ray structure of **1** (Figure S11), which has a triclinic unit cell ($a = 9.6483$, $b = 10.7101$, $c = 13.9602$ Å; $\alpha = 100.241$, $\beta = 107.743$, $\gamma = 94.394°$) with one molecule in the P1 space group.[3a] The unit cell volume of the PXRD structure (3799.47 Å^3) is three times larger than that of the single-crystal structure (1338.83 Å^3), although the constituent foldamers have nearly identical backbone conformations, as shown in the backbone overlaid structure (RMSD 0.627 Å, 24 pairs of backbone atoms; Figure 3a). The different orientation of the C-terminus benzyl group and differences in the crystal systems and intermolecular packing motifs may be attributed to the single crystal growing under equilibrium conditions, whereas the formation of foldectures occurred rapidly under non-equilibrium conditions.

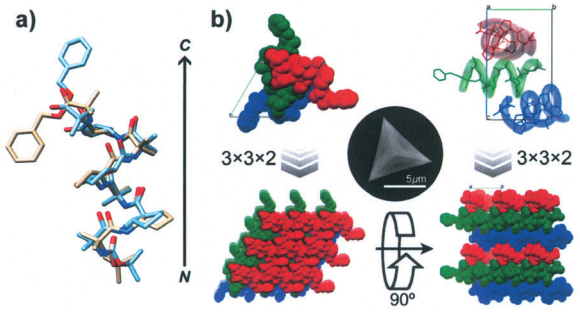

Figure 3. Relationship between foldamer conformation, molecular packing motif and foldecture morphology. a) Overlay of PXRD (light blue) and single crystal[3a] (beige) foldamer geometries showing similar 11-helical secondary structures (magenta ribbon). b) Molecular packing motif of foldectures in the unit cell (top left and right), and extended molecular network (bottom left and right). Individual α/β-heptamer molecules in the unit cell are shown in red, green, blue colors. The center circle shows a SEM image of foldecture $\mathbf{F}_3$.

The molecular packing motif of **1** is shown in Figure 3b (top left and right). Three foldamer molecules (colored in red, green, and blue) pack through a combination of hydrogen bonding and hydrophobic interactions. The molecular networks generated from a view along the *a*- and *c*-axes (Figure 3b bottom left and right, respectively; Supporting Information movie), reveal a layer-by-layer parallel packing of foldamers in the unit cell. The three crystallographically equivalent foldamers in the unit cell are arrayed head-to-tail in a helix along a 3-fold screw axis parallel to the [001] direction. The angle between helical axes is approximately 120 degrees, thus creating a triangular network that recapitulates the unique trigonal symmetry of foldectures $\mathbf{F}_{0-4}$ with surprising fidelity. The unexpected similarities between the molecular-level and microscale symmetries suggest that the molecular packing mode influences the formation of the unique trigonal shapes observed for $\mathbf{F}_{0-4}$. Furthermore, the tail of $\mathbf{F}_1$ was determined to extend from the [001] direction, based on the refined March–Dollase preferred orientation parameter ($P_{MD} = 1.2$) in the Bragg–Brentano geometry system of the PAL 9B HRPD Synchrotron Beamline (Figure S10).[14,15] This molecular-level structural analysis provides a potential link between the 3-fold screw axis and the unique trigonal shape of the foldecture and allows a rationalization as to why the morphologies are distinct from those of 4-fold symmetric foldectures derived from 12-helical peptides (Figure S12).

As revealed by TEM analysis (inset of Figure 2d), the unexpected hollow interior of $\mathbf{F}_3$ attracted our attention owing to its similarity to BMCs and potential utility as a large-scale molecular container capable of delivering an efficacious quantity of guest molecule. The cavity volume is estimated to about 7 μm^3, which is approximately 2000 times larger than a BMC (Figure S14). To investigate the encapsulation ability of $\mathbf{F}_3$, self-assembly studies were performed in the presence of three different types of fluorescent guest materials: quantum dots (green), Rhodamine B (red), and green fluorescent protein (GFP) (Supporting Information). Analysis of the resulting assemblies by confocal laser scanning microscopy (CLSM) revealed that all of the fluorescent guest materials were successfully encapsulated in $\mathbf{F}_3$ (Figure 4a–c and Figure S16), whereas no fluorescent signal was observed in control experiments (Figure S15). The 3D volume reconstructed by Z-stack analysis at 1 μm of focal length intervals provides direct evidence for the existence of a central cavity in $\mathbf{F}_3$ that encapsulates Rhodamine B (Figure 4d and Figure S17).[16] Host foldectures containing the fluorescent guests have morphologies identical to the empty cohort, implying that the guests neither impede nor template the self-assembly behavior of **1**. Encapsulated Rhodamine B can be released in acidic media by taking advantage of the acid-labile Boc group of **1**. Upon treatment with 2 N HCl solution, the appearance of

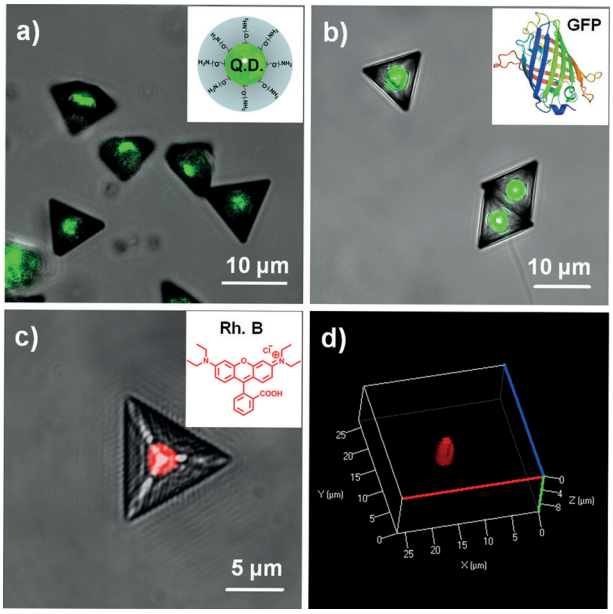

Figure 4. CLSM images of encapsulated fluorescent materials in the cavity of foldecture $\mathbf{F}_3$. a) Green fluorescent quantum dot. b) Green fluorescent protein (GFP). c) Rhodamine B. d) 3D Z-stack image of Rhodamine B situated within the foldecture cavity.

a pinhole on the basal face of $\mathbf{F_3}$ was observed. The basal face gradually disintegrated to form $\mathbf{F_4}$-like shapes over a 24 hour period (Figures S18 and S19). The unexpected difference in hydrolysis rates likely reflects a face-specific molecular arrangement conserved in $\mathbf{F_3}$ and $\mathbf{F_4}$, resulting from anisotropic molecular packing. Although the exact mechanism for the formation of the void space remains unresolved (Figure S13), the guest-independent property makes these hollow foldectures ideally suitable for the development of biocompatible delivery vehicles and containment vessels.

In summary, we have shown that the 11-helical foldamer **1** self-assembles to reproducibly form a new set of foldectures $\mathbf{F_0}$–$\mathbf{F_4}$ with unique trigonal bipyramid-based morphologies. High-resolution PXRD analysis of the foldecture packing motif provided an important link between the molecular-level symmetry and the microscale morphology. The 3-fold symmetrical shapes observed from the self-assembly of **1** are distinct from the 4-fold symmetrical shapes generated from 12-helical foldamers, implying that foldamer secondary structure constrains the symmetry elements in foldecture shape and that new and useful foldecture shapes may be available from other peptide secondary structures. Along with these fundamental studies, we also demonstrated the utility of foldectures with hollow interiors to serve as robust and very large supramolecular hosts for inorganic, organic, and even protein guests. We believe this work will pave the way for the design of functional foldectures with greater 3D shape diversity.

Acknowledgements

This work was supported by Basic Science Research Programs through NRF grant (2013R1A2A1A01008358, 2009-0083525) funded by the Korea government (MSIP). The authors also acknowledge PAL for beamline use.

Keywords: foldamers · hollow nanostructures · host–guest systems · molecular architecture · self-assembly

How to cite: *Angew. Chem. Int. Ed.* **2015**, *54*, 13204–13207
Angew. Chem. **2015**, *127*, 13402–13405

[1] a) S. Kwon, A. Jeon, S. H. Yoo, I. S. Chung, H.-S. Lee, *Angew. Chem. Int. Ed.* **2010**, *49*, 8232–8236; *Angew. Chem.* **2010**, *122*, 8408–8412; b) S. Kwon, H. S. Shin, J. Gong, J.-H. Eom, A. Jeon, S. H. Yoo, I. S. Chung, S. J. Cho, H.-S. Lee, *J. Am. Chem. Soc.* **2011**, *133*, 17618–17621; c) S. Kwon, K. Kang, A. Jeon, J. H. Park, I. Choi, H.-S. Lee, *Tetrahedron* **2012**, *68*, 4368–4373; d) J. Kim, S. Kwon, S. H. Kim, C.-K. Lee, J.-H. Lee, S. J. Cho, H.-S. Lee, H. Ihee, *J. Am. Chem. Soc.* **2012**, *134*, 20573–20576; e) S. H. Yoo, T. Eom, S. Kwon, J. Gong, J. Kim, S. J. Cho, R. W. Driver, Y. Lee, H. Kim, H.-S. Lee, *J. Am. Chem. Soc.* **2015**, *137*, 2159–2162.

[2] a) S. H. Gellman, *Acc. Chem. Res.* **1998**, *31*, 173–180; b) R. P. Cheng, S. H. Gellman, W. F. DeGrado, *Chem. Rev.* **2001**, *101*, 3219–3232; c) D. Seebach, J. Gardiner, *Acc. Chem. Res.* **2008**, *41*, 1366–1375; d) W. S. Horne, S. H. Gellman, *Acc. Chem. Res.* **2008**, *41*, 1399–1408; e) T. A. Martinek, F. Fülöp, *Chem. Soc. Rev.* **2012**, *41*, 687–702.

[3] a) S. H. Choi, I. A. Guzei, L. C. Spencer, S. H. Gellman, *J. Am. Chem. Soc.* **2008**, *130*, 6544–6550; b) M. A. Schmitt, S. H. Choi, I. A. Guzei, S. H. Gellman, *J. Am. Chem. Soc.* **2005**, *127*, 13130–13131; c) A. Hayen, M. A. Schmitt, F. N. Ngassa, K. A. Thomasson, S. H. Gellman, *Angew. Chem. Int. Ed.* **2004**, *43*, 505–510; *Angew. Chem.* **2004**, *116*, 511–516.

[4] a) J. M. Shively, F. Ball, D. H. Brown, R. E. Saunders, *Science* **1973**, *182*, 584–586; b) T. O. Yeates, M. C. Thompson, T. A. Bobik, *Curr. Opin. Struct. Biol.* **2011**, *21*, 223–231.

[5] a) C. A. Kerfeld, M. R. Sawaya, S. Tanaka, C. V. Nguyen, M. Phillips, M. Beeby, T. O. Yeates, *Science* **2005**, *309*, 936–938; b) S. Tanaka, C. A. Kerfeld, M. R. Sawaya, F. Cai, S. Heinhorst, G. C. Cannon, T. O. Yeates, *Science* **2008**, *319*, 1083–1086.

[6] a) T. O. Yeates, Y, Tsai, S. Tanaka, M. R. Sawaya, C. A. Kerfeld, *Biochem. Soc. Trans.* **2007**, *35*, 508–511; b) T. O. Yeates, C. A. Kerfeld, S. Heinhorst, G. C. Cannon, J. M. Shively, *Nat. Rev.* **2008**, *6*, 681–691; c) S. Tanaka, M. R. Sawaya, T. O. Yeates, *Science* **2010**, *327*, 81–84; d) S. Cheng, Y. Liu, C. S. Crowley, T. O. Yeates, T. A. Bobik, *BioEssays* **2008**, *30*, 1084–1095; e) M. Takenoya, K. Nikolakakis, M. Sagermann, *J. Bacteriol.* **2010**, *192*, 6056–6063.

[7] a) N. P. King, W. Sheffler, M. R. Sawaya, B. S. Vollmar, J. P. Sumida, I. André, T. Gonen, T. O. Yeates, D. Baker, *Science* **2012**, *336*, 1171–1174; b) N. P. King, J. B. Bale, W. Sheffler, D. E. McNamara, S. Gonen, T. Gonen, T. O. Yeates, D. Baker, *Nature* **2014**, *510*, 103–108.

[8] a) B. Wörsdörfer, K. J. Woycechowsky, D. Hilvert, *Science* **2011**, *331*, 589–592; b) Y.-T. Lai, D. Cascio, T. O. Yeates, *Science* **2012**, *336*, 1129; c) Y.-T. Lai, E. Reading, G. L. Hura, K.-L. Tsai, A. Laganowsky, F. J. Asturias, J. A. Tainer, C. V. Robinson, T. O. Yeates, *Nat. Chem.* **2014**, *6*, 1065–1071.

[9] a) F. Boato, R. M. Thomas, A. Ghasparian, A. Freund-Renard, K. Moehle, J. A. Robinson, *Angew. Chem. Int. Ed.* **2007**, *46*, 9015–9018; *Angew. Chem.* **2007**, *119*, 9173–9176; b) J. M. Fletcher, R. L. Harniman, F. R. H. Barnes, A. L. Boyle, A. Collins, J. Mantell, T. H. Sharp, M. Antognozzi, P. J. Booth, N. Linden, M. J. Miles, R. B. Sessions, P. Verkade, D. N. Woolfson, *Science* **2013**, *340*, 595–599; c) H. Gradišar, S. Božič, T. Doles, D. Vengust, I. Hafner-Bratkovič, A. Mertelj, B. Webb, A. Šali, S. Klavžar, R. Jerala, *Nat. Chem. Biol.* **2013**, *9*, 362–366.

[10] a) K. Matsuura, K. Murasato, N. Kimizuka, *J. Am. Chem. Soc.* **2005**, *127*, 10148–10149; b) K. Matsuura, K. Watanabe, T. Matsuzaki, K. Sakurai, N. Kimizuka, *Angew. Chem. Int. Ed.* **2010**, *49*, 9662–9665; *Angew. Chem.* **2010**, *122*, 9856–9859.

[11] a) Y.-S. Yoo, J.-H. Choi, N.-K. Oh, W.-C. Zin, S. Park, T. Chang, M. Lee, *J. Am. Chem. Soc.* **2004**, *126*, 6294–6300; b) J.-H. Ryu, H.-J. Kim, Z. Huang, E. Lee, M. Lee, *Angew. Chem. Int. Ed.* **2006**, *45*, 5304–5307; *Angew. Chem.* **2006**, *118*, 5430–5433.

[12] A. Le Bail, H. Duroy, J. L. Fourquet, *Mater. Res. Bull.* **1988**, *23*, 447–452.

[13] a) P. Thompson, D. E. Cox, J. B. Hastings, *J. Appl. Crystallogr.* **1987**, *20*, 79–83; b) L. B. McCusker, C. Baerlocher, *Chem. Commun.* **2009**, 1439–1451.

[14] W. A. Dollase, *J. Appl. Crystallogr.* **1986**, *19*, 267–272.

[15] a) J. Ihringer, A. Kuster, *J. Appl. Crystallogr.* **1993**, *26*, 135–137; b) D. Kriegner, Z. Matěj, R. Kužel, V. Holý, *J. Appl. Crystallogr.* **2015**, *48*, 613–618.

[16] a) B. R. Masters, G. Gonnord, P. Corcuff, *J. Microsc.* **1997**, *185*, 329–338; b) D. Bucher, M. Scholz, M. Stetter, K. Obermayer, H.-J. Pflüger, *J. Neurosci. Methods* **2000**, *100*, 135–143; c) B. Gligorijevic, R. McAllister, J. S. Urbach, P. D. Roepe, *Biochemistry* **2006**, *45*, 12400–12410; d) J. Huo, M. Marcello, A. Garai, D. Bradshaw, *Adv. Mater.* **2013**, *25*, 2717–2722.

Received: May 9, 2015
Revised: July 13, 2015
Published online: August 27, 2015

